Valency Neutron Capture in ^{92}Mo(n,γ)^{93}Mo†

O. A. Wasson
Oak Ridge National Laboratory, Oak Ridge, Tennessee 37830, and Brookhaven National Laboratory, Upton, New York 11973

and

G. G. Slaughter
Oak Ridge National Laboratory, Oak Ridge, Tennessee 37830

(Received 21 August 1972)

Capture γ-ray spectra from the ^{92}Mo(n,γ)^{93}Mo reaction were measured for neutron energies below 100 keV using the 10-m flight path at the Oak Ridge electron linear accelerator. For neutron energies less than 25 keV a total of 23 different s- and p-wave resonances were resolved. The neutron binding energy is 8067.4± 1.5 keV. The partial radiation widths for the 12 highest energy γ rays which populate positive-parity states below 2.5-MeV excitation were deduced and compared to the valency-model predictions of Lane and Lynn. For γ-ray energies less than 6.5 MeV, the average $M1$ partial radiation width is approximately equal to the average $E1$ partial radiation width. The reduced transition strengths as defined by Bartholomew for these transitions are $\bar{k}(E1) = (1.2 \pm 0.2) \times 10^{-3}$ and $\bar{k}(M1) = (11.5 \pm 2.3) \times 10^{-3}$. For the 7126-keV transition to the $s_{1/2}$ first excited state the average reduced strength is enhanced by a factor of 5 and 2 for the $E1$ and $M1$ transitions, respectively. Nearly 30% of this enhancement for the $E1$ multipoles is attributed to the valency-model contribution while the remainder is assigned to other processes such as the giant dipole resonance and doorway-state components. The average $E2$ width for the 8067-keV ground-state γ rays is approximately 10% of the average $E1$ ground-state width.

I. INTRODUCTION

One of the more interesting developments in the field of radiative neutron capture is the observation of the importance of single-particle or valency components in the electric-dipole γ-ray decays for nuclei near the peak of the $3p$ giant resonance in the neutron strength function. The Brookhaven chopper group[1] observed that the γ-ray spectra from neutron capture into strong p-wave resonances in the target nucleus ^{98}Mo were in remarkable agreement with the single-particle or valency model of Lane and Lynn.[2,3] However, for measurements at higher neutron energies which were done at the Oak Ridge electron linear accelerator in collaboration with G. G. Slaughter, the valency-model contribution was reduced. This was due to the smaller p-wave reduced neutron widths at these energies.[4] Large valency-model contributions have also been reported[5,6] for p-wave neutron capture for several resonances in the target nuclei ^{96}Zr and ^{108}Pd.

The Brookhaven group[1] also reported significant single-particle components for radiative neutron capture in several groups of unresolved resonances in the target nucleus ^{92}Mo. Single-particle effects are expected to be important in this nucleus since there is neutron shell closure for the target nucleus, and the ground state of the product nucleus, ^{93}Mo, contains a single neutron in the $d_{5/2}$ orbital. The purpose of the present work is to report a detailed test of the predictions of the valency model using the higher neutron energy-resolution capture γ-ray measurements performed at the Oak Ridge electron linear accelerator (ORELA).[7]

II. EXPERIMENTAL DETAILS

The source of pulsed neutrons for this experiment was the Oak Ridge electron linear accelerator (ORELA), an L-band (1300-MHz) machine dedicated to neutron time-of-flight measurements. ORELA accelerates electrons to a nominal energy of 140 MeV, and is capable of 15-A pulses (at a pulse width of 24 nsec or less) at a maximum repetition rate of 1000/sec, for 50-kW maximum on a water cooled and moderated tantalum target. At maximum beam current and optimum pulse width (24–30 nsec) the neutron production (through the γ-n reaction) is 10^{11}/pulse, or 10^{14} neutrons/sec, time average at the maximum repetition rate of 1000/sec. The flight tube shares the target-room vacuum (about 3 Torr) and contains 1.5- and 0.3-m-long shadow shields to block the direct view of the tantalum target from the sample. The beam is collimated to a nominal 10-cm diam at the 10.4-m sample location.

The 238-g metallic-molybdenum-powder sample was enriched to 97.37% ^{92}Mo. The sample was

mounted in a cylindrical container of silicon dioxide, with an inside diameter of about 7.0 cm and a sample length of about 7.0 cm, resulting in a sample thickness of ~0.0407 atoms/b.

The γ-ray detector is a 37-cm^3 ORTEC true coaxial Ge(Li) crystal in a vertical-mount cryostat, positioned directly under the sample. A TC-135 preamplifier with analog, common-mode, and fast-timing outputs is attached directly to the cryostat. The analog and common-mode outputs drive a 107-m Twin-Ax cable (RG-22B/U) to the differential inputs of a TC-200 amplifier in the laboratory upstairs. This combination reduces the rf pickup to a negligible amount. The timing output is conditioned by an ORTEC 454 timing filter amplifier, which provides amplitude and rise-time compensated pulses to an ORTEC 453 constant fraction timing discriminator. The fast NIM-logic-pulse output of this discriminator is carried upstairs by 107 m of RG-214/U cable. All of the above equipment is housed in a 1.8-m-long by 1.1-m-wide by 2.0-m-high shield made of copper screen on a sheet-metal floor. This shield attenuates the electromagnetic pickup from the accelerator-beam current pulse, and permits the fast timing decision to be made in a quiet environment.

The γ flash from the target is undoubtedly attenuated tremendously by the shadow shield, and is alleviated somewhat by the back angle of the flight path with respect to the electron beam (105°). Indeed, the pulse-height spectrum of the γ-flash pulses shows that they are predominantly low-energy γ rays, evidently as a result of large-angle Compton scattering. However, the γ-flash contribution per accelerator pulse must be kept very low in amplitude (less than the resolution of the detector) or low in probability of occurrence, or both. The TC-200 is operated at a baseline pulse width of 6 to 8 μsec, so any appreciable contribution from the γ flash will affect the resolution of γ-ray events down to an incident neutron energy of about 10 keV. In practice, enough Pb was put into the beam to reduce any noticeable contribution from the γ flash to one pulse in three. For the present experiment, 6.3 cm of lead was required. The crystal was shielded with 10 cm of lead in the horizontal plane, and 5.4 cm of ^{6}LiH were used between the sample and the crystal.

The analog pulses from the TC-200 output were digitized by an 8192-channel 100-MHz Nuclear Data Series 2200 analog-to-digital converter. The timing pulses out of the constant fraction timing discriminator were digitized by a 10-nsec 131 072-channel TMC TF-440-10 clock. The digitizers were interlocked so as to maintain the correlation between events. The digital information is transmitted through ground isolators to one of two SEL 810B computers (16 bits, 16 000 core memory, 0.75-μsec cycle time) which has either a 400 000 or an 800 000 word-addressable fixed-head disk associated with it. A routine called CRUNCH, which is peculiar to each of the four simultaneous experiments on the computer, compares the two data words of an event to the experiment parameters which are stored at the beginning of the disk area.

The routine determines what is to be done with the event, and reduces the two data words to an address on the disk (track number and track position). The proper location in the proper area is updated by means of a system of address and data buffers and block transfer controllers connecting the disk to the computer.[7] A total of 361 215 channels was used for the present experiment in the following manner: 768 channels for experiment parameters; 79 groups of 4096 pulse-height channels, each of which corresponded to a resonance (47 groups) or a background interval (32 groups); 32 767 channels for time-of-flight singles spectrum; and 4096 channels for pulse-height singles spectrum. The neutron energy range was from 0.005 to 90 keV, and the γ-ray energy range was from 0.203 to 8.7 MeV. The present experiment was run with the detector at 90° to the neutron beam for a total of 7977.7 kWh on the target. Another experimental run was made with the detector at 140° to the neutron beam for a total of 6156 kWh on the target. This run was used to determine resonance spins from the γ-ray angular distribution. A 0.25-mm gold foil was run in conjunction with the ^{92}Mo sample for finding absolute γ-ray partial widths, using the known partial widths in the 4.9-eV gold resonance as a standard. The neutron flux was measured by the time-of-flight spectrum from a ^{10}B slab sample. The relative efficiency of the crystal as a function of energy was measured by the ^{14}N$(n,\gamma)^{15}$N reaction using a Be_3N_2 sample, and a ^{226}Ra source.

III. THEORETICAL PREDICTIONS

The valency model of radiative neutron capture as reported by Lynn[3] predicts that the γ-ray decay width for an $E1$ multipole from the neutron-capturing resonance λ to a low-lying final state j is given by

$$\Gamma_{\gamma\lambda j} = \left(\frac{E_\gamma}{\hbar c}\right)^3 \times I_{\lambda j}{}^2 \times \theta_\lambda{}^2 \times \theta_j{}^2 \frac{|(j' I J_\lambda \| Y^{(1)} \| j'' I J_j)|^2}{2J_\lambda + 1}, \quad (1)$$

where the first factor contains the γ-ray energy dependence, and the second factor is the single-particle matrix element. The third and fourth fac-

tors are the dimensionless reduced neutron widths of the capturing and final states, respectively. These factors measure the amount of single-particle neutron component in the respective states. The final factor is the reduced matrix element which contains the angular momentum factors. For p-wave neutron capture ($l_n=1$) in the even-even target nucleus ^{92}Mo the correct expression for the reduced matrix element is given by

$$\frac{|\langle J_\lambda 0\, J_\lambda \| Y^{(1)} \| J_j 0\, J_j\rangle|^2}{2J_\lambda+1}=\frac{9}{4\pi}(2J_j+1)^2W^2(J_\lambda J_\lambda J_j J_j;01)\times W^2(1J_\lambda l_j J_j;\tfrac{1}{2}1)C_{11}^{\,2}(l_j 0;00)\,, \tag{2}$$

where J_λ is the capturing-state spin, J_j is the final-state spin, l_j is the orbital angular momentum of neutron in final state, W is the Racah coefficient, and C is the Clebsch-Gordan coefficient.

The single-particle radial matrix element, which is given by

$$I_{\lambda j}^{\,2}=\tfrac{16}{9}\pi\bar{e}^2\left|\int_0^\infty U_\lambda U_j r\,dr\right|^2, \tag{3}$$

has been evaluated by Lynn[3] for neutron wave functions in an Eckart potential with the well radius adjusted so that the initial single-particle state λ was just bound. Here $\bar{e}$ is the neutron effective charge which is assumed to be given by

$$\bar{e}=eZ/A$$

in the present work.

The dimensionless reduced neutron width of the capturing state, which is the width relative to the Wigner limit,[8] is given by

$$\theta_{\lambda n}^{\,2}=\Gamma_{\lambda n}/(2P_c\hbar^2/Ma^2)\,,$$

where $\Gamma_{\lambda n}$ is the neutron width of resonance, a is the nuclear radius which is 6.7 fm for this experiment, M is the neutron mass, and $P_c=[1+(ka)^2]/(ka)^3$ is the p-wave neutron penetrability. For the final state we use

$$\theta_j^{\,2}=S_{1j}$$

which is the spectroscopic factor deduced in (d,p) experiments.

In order to evaluate the partial radiation widths for p-wave neutron capture in ^{92}Mo the following nuclear parameters are required:

(1) $\Gamma_{\lambda n}$, the neutron width of each resonance;
(2) J_λ^π, spin and parity of neutron resonance;
(3) $\Gamma_{\lambda\gamma}$, the total radiation width of each resonance;
(4) J_j^π, spin and parity of final state;
(5) S_{1j}, neutron spectroscopic factor of final state;
(6) l_j, the single-particle orbital in the final state.

The neutron resonance parameters were mostly unknown previously, but have been determined from combining the present capture γ-ray measurement with neutron-transmission and total-capture results from another experiment.[9] The parameters of the low-lying states in ^{93}Mo are known from a large variety of charged-particle reactions.[10-18] The spectroscopic factors used in the present analysis are taken from the work of Moorhead and Moyer[11] using the $\frac{5}{2}^+$ spin assignment for the 1691-keV state in ^{93}Mo as deduced by Ball.[16] The partial radiation widths are calculated using these parameters and are compared with the experimentally observed widths in a later section.

IV. MEASUREMENT OF PARTIAL RADIATION WIDTHS

A. Measurement of γ-Ray Peak Areas

The partial radiation widths are determined from the γ-ray peak areas in the γ-ray spectra using the expression

$$\Gamma_{\gamma\lambda j}=\frac{A_{\lambda j}\Gamma_{\lambda\gamma}P_{\lambda j}}{\epsilon_j N_\lambda}, \tag{4}$$

where λ and j label capturing and final states, respectively; k is a normalizing factor determined to the 3169-eV resonance; $A_{\lambda j}$ is the γ-ray peak area; $\Gamma_{\lambda\gamma}$ is the total radiation width of resonance λ; ϵ_j is the relative detector efficiency; N_λ is the number of neutrons captured in resonance λ; and $P_{\lambda j}$ is the angular-distribution factor. Now $N_\lambda=B_\lambda\varphi(E)$, where $\varphi(E)$ is the incident neutron flux and B_λ is the capture area per unit neutron flux.

The γ-ray net peak areas for each of the three peaks produced by the Ge(Li) detector for each high-energy γ ray ($E_\gamma>4.0$ MeV), as well as the single peak produced by the low-energy γ rays, were obtained by subtracting from each peak a linear background fitted to a neighboring off-peak region for each spectrum. The errors recorded are those due to statistical uncertainty in the net peak areas. For the high-energy γ rays the two-photon and one-photon escape peak areas were summed while the full-energy peak areas were used for the low-energy γ rays.

B. Detector Efficiency and γ-Ray Energy Calibration

The relative γ-ray detection efficiency ϵ_j was determined for the γ-ray energy interval $2<E_\gamma<11$ MeV from the γ rays from the ^{14}N$(n,\gamma)^{15}$N reaction from a Be_3N_2 sample. The efficiency for the interval $0.5<E_\gamma<4$ MeV was obtained from a ^{226}Ra source. Both samples were placed in the ^{92}Mo-sample position. The efficiencies of the high-energy γ rays from low-energy neutron capture in

nitrogen were determined using the absolute intensities of Thomas, Blatchley, and Bollinger.[19] The efficiency for the low-energy γ rays ($E_\gamma < 2.4$ MeV) from the Ra source was obtained using the γ-ray intensities of Dickens.[20] After fitting smooth curves to both data sets, the full-energy curves of both sets were normalized at 1.8 MeV to produce the final efficiency curve used in the calculations.

A test of the precision of the relative efficiency between 0.94 and 7.12 MeV was done using the two-step γ-ray cascade from the capturing state through the first excited state to the ground state in ^{93}Mo. Since the internal conversion coefficients for these two γ rays are small, the intensity of the 0.94-keV γ ray should equal or exceed that of the 7.1-MeV γ ray in all spectra. This relationship was observed to be valid within statistical error for all the γ-ray spectra.

The energies of the ^{93}Mo γ rays were determined by known γ rays internal to the data set. The wide, low-neutron-energy background γ-ray spectrum included prominent lines from pair annihilation and capture γ rays from hydrogen and iron. Since there was no need in the present experiment for high-γ-ray-energy precision the low-energy γ rays are determined to an error of ±1 keV while the high-energy γ rays have an error of ±2 keV. The neutron binding energy is measured to be 8067.4 ± 1.5 keV from the combination of the primary and secondary γ-ray energies which sum to the binding energy.

C. Number of Neutrons Captured

One of the largest sources of uncertainty in past resonant-neutron-capture γ-ray experiments was the method used to determine the number of neutrons captured in each neutron resonance. The method generally used is to assume that the summed γ-ray spectrum over a wide γ-ray-energy interval is proportional to the number of neutrons captured. This method should be most precise for complicated γ-ray spectra. In the present experiment we first used the same method. Here we have assumed that the total spectral counts observed in the γ-ray-energy interval from 2.3 to 3.5 MeV, T_λ, is proportional to the number of neutrons captured, independent of neutron energy. In this case

$$N_\lambda = T_\lambda - B,$$

where B is the background contribution deduced from an off-resonance region. The background contributions varied from 10 to 90%. For neutron energies exceeding 25 keV, there is no off-resonance region and the error in the background estimate is large.

As a check on the reliability of using the above procedure we also calculated the number of neutrons captured in each neutron-energy interval. The incident-neutron flux for each neutron-energy interval was measured using the ^{10}B$(n, \alpha\gamma)^7$Li reaction in a thick ^{10}B sample. The capture yield for each interval was calculated by the Monte-Carlo program O5R[21] using the neutron resonance parameters reported in another publication.[9] This program includes the effects of multiple neutron scattering, Doppler broadening, and resonance self-protection. For resonances of unknown total radiation width, a value of 0.170 eV was used. For resonances unresolved in the capture-γ-ray spectral measurement, the summed areas of the individual resonances were used.

The ratio of the summed spectral area to the calculated number of captures is shown in Fig. 1. The points represent the various γ-ray spectra which in some cases include several neutron resonances. The error bars indicate the estimated ±15% precision of the calculated captures as well as an estimate of the background error. The horizontal line indicates the mean value for the 20 points for $E_n < 15$ keV. The scatter of the points about the mean value is described by a relative standard deviation of 22%, which is an indication of the precision of the two methods of determining the number of neutrons captured. A systematic rise in the points is observed for higher neutron energies which we attribute to an uncorrected background contribution to the net spectral counts. We have used the calculated number of captured neutrons to calculate the partial radiation widths for neutron energies less than 25 keV, for which we estimate the systematic error to be less than 25%. For higher neutron energies, where the resonances are unresolved, we have used the net spectral counts as a measure of the captures. The system-

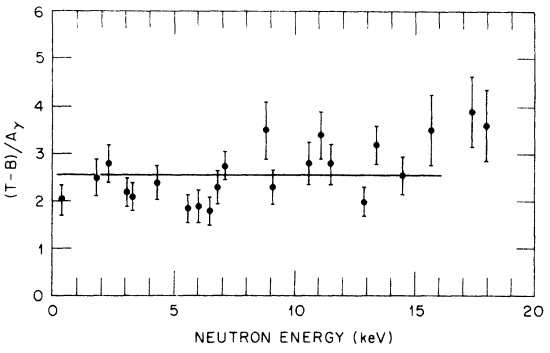

FIG. 1. Ratio of the summed γ-ray spectral counts to calculated number of neutron captures for the various γ-ray spectra.

atic error is much larger in this region because of the large background uncertainty.

D. Correction for γ-Ray Angular Distribution

The γ-ray spectra used to deduce partial radiation widths were obtained at 90° with respect to the incident neutron beam. For resonances of spin $\frac{1}{2}$ the γ-ray angular distribution is isotropic.[22] For spin $\frac{3}{2}$ resonances the distribution is not isotropic and a correction factor must be applied to the 90° measurement in order to determine the partial width. The factors $P_{\lambda j}$ by which the observed γ-ray peak area must be multiplied to correct for the angular distribution are listed in Table I. The factor $P_{\lambda j}$ is given by

$$P_{\lambda j} = \int I(\theta) d\Omega / 4\pi I(90°) ,$$

where $I(\theta)$ is the angular-distribution factor normalized so that

$$\int I(\theta) d\Omega = 1 .$$

This factor was applied to all transitions using the spins and parities listed in Table IV.

E. Absolute Partial Widths Relative to Gold

The absolute values of the partial radiation widths in ^{93}Mo were determined relative to the high-energy γ-ray intensities in the 4.9-eV resonance in gold. A separate run was taken using a composite sample of ^{92}Mo and Au. The sample properties and experimental results are listed in Table II. The 7126-keV γ-ray width in the 3169-eV resonance of ^{92}Mo was normalized to the sum of the high-energy γ-ray widths for the 4.9-eV resonances in gold as measured by Kane.[23] Kane's result for the intensity $(\Gamma_{\lambda j}/\Gamma_{\lambda\gamma})$ of these γ rays is 0.1334 photons per capture. The relative neutron flux for the two resonances was measured using the $^{10}B(n, \alpha\gamma)^{7}Li$ reaction from a 2.59-g/cm^2 ^{10}B sample, while the number of captured neutrons was calculated from the known resonance parameters using the above-mentioned computer program.[21] The partial width for the 7126-keV γ ray in the 3169-eV resonance, as deduced from applying Eq. (4) to both resonances, is 0.064 eV. This number then determines the value of the constant k in Eq. (4) which is used for the other spectra in ^{93}Mo.

The 3169-eV s-wave resonance was chosen for the normalization with gold because it is the lowest-energy resonance for which the radiation width was known. A correction for the approximate 15% contribution from captures in the 3061-eV resonance was applied as is discussed more completely in a later section. The total radiation widths of the four lowest-energy resonances have not been deduced because of their small neutron widths. If we assume that the total radiation width of the 347-eV s-wave resonance is equal to the average s-wave width and normalize this spectrum to the gold standard, we obtain widths within 10% of those obtained from the 3169-eV resonance.

V. EXPERIMENTAL RESULTS

The γ-ray counting rate as a function of neutron flight time is shown in Fig. 2. Included are those events which deposit more than 203-keV energy in the detector. The histogram below the spectrum indicates the contiguous gates selected to record γ-ray spectra. The energies of the neutron resonances are indicated above each peak. No resonances were resolved for neutron energies greater than 25 keV while a total of 23 resonances were resolved for lower energies. The weak peaks at neutron energies below 2 keV are assigned to other molybdenum isotopes in the sample.

As representative examples, the low-energy part of the γ-ray spectrum is shown for two reso-

TABLE I. γ-ray angular distribution $I(\theta)$ and correction factor $P_{\lambda j}$ for dipole γ rays. The capturing and final-state spins are labeled by J_λ and J_j, respectively.

	$P_{\lambda j}$, $I(\theta)$	
J_j	$J_\lambda = \frac{1}{2}$	$J_\lambda = \frac{3}{2}$
$\frac{1}{2}$	$1, 1/4\pi$	$\frac{4}{5}, (1/16\pi)(2+3\sin^2\theta)$
$\frac{3}{2}$	$1, 1/4\pi$	$\frac{5}{4}, (1/20\pi)(7-3\sin^2\theta)$
$\frac{5}{2}$		$\frac{20}{21}, (3/80\pi)(6+\sin^2\theta)$

TABLE II. Parameters and data used for partial-radiative-width normalization.

Parameter	Gold	^{92}Mo
Mass (g/cm^2)	0.472	6.215
E_r (eV)	4.906	3169
Γ_n (eV)	0.015 72	7.8
Γ_γ (eV)	0.124	0.210
g	0.625	1.0
E_j (MeV)	6.2-6.6	7.126
$\varphi(E)$	550 ± 15	2.98 ± 0.10
I_j	0.1334	
A_n	1.27	2.48
% multiple scattering	9.9	30
A_j	7639 ± 180	221 ± 22

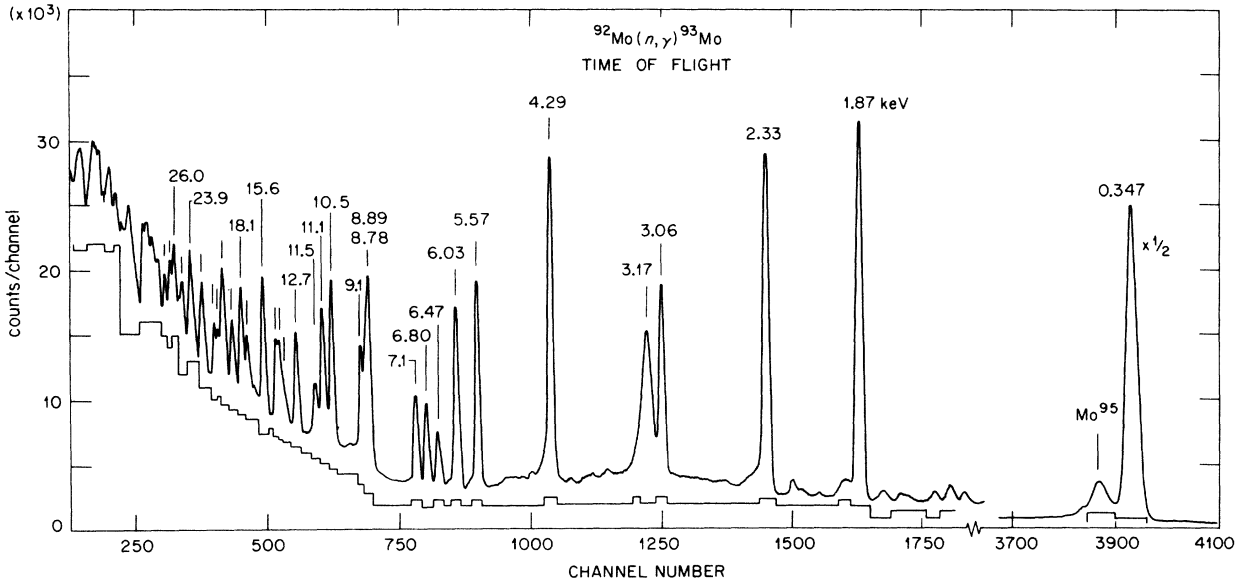

FIG. 2. Neutron time-of-flight spectrum. The histogram indicates the contiguous gates used to record γ-ray spectra.

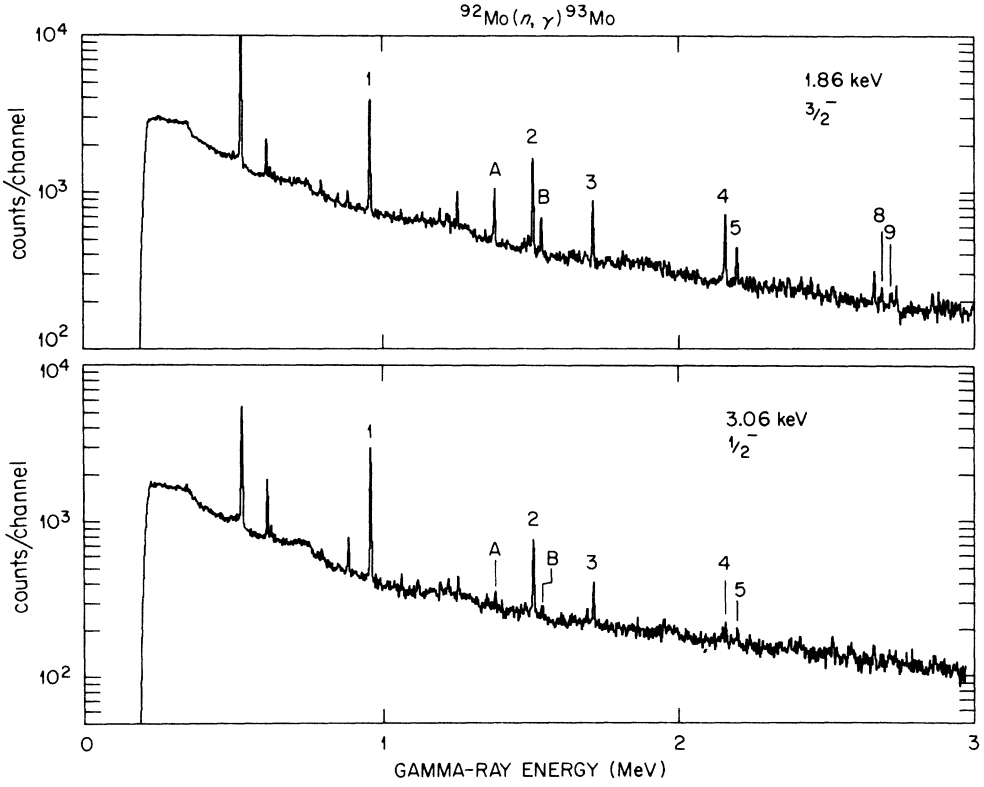

FIG. 3. Representative low-energy γ-ray spectra. The numbered peaks are transitions to the ground state while the lettered peaks are transitions to other states. The unlabeled peaks are background.

nances in Fig. 3. The labeled peaks indicate the capture γ rays for ^{93}Mo while the remaining peaks are due to other processes. The numbered peaks are identified as secondary transitions populating the ground state. The lettered peaks populate other states. These γ rays are not primary transitions from the capturing state since their energy does not increase with increasing neutron energy. It is shown later that a large fraction of the intensity of these γ rays results from the second part of two-step γ-ray decays from the capturing state to the ground state. Thus we have been unable to deduce the spins of the neutron resonances from the relative strength of the low-energy γ rays as has been done for more complicated nuclei.[24]

Figure 4 shows representative spectra for the high-energy γ rays from four resonances. The γ-ray-energy interval extends from 4 to 8.3 MeV.

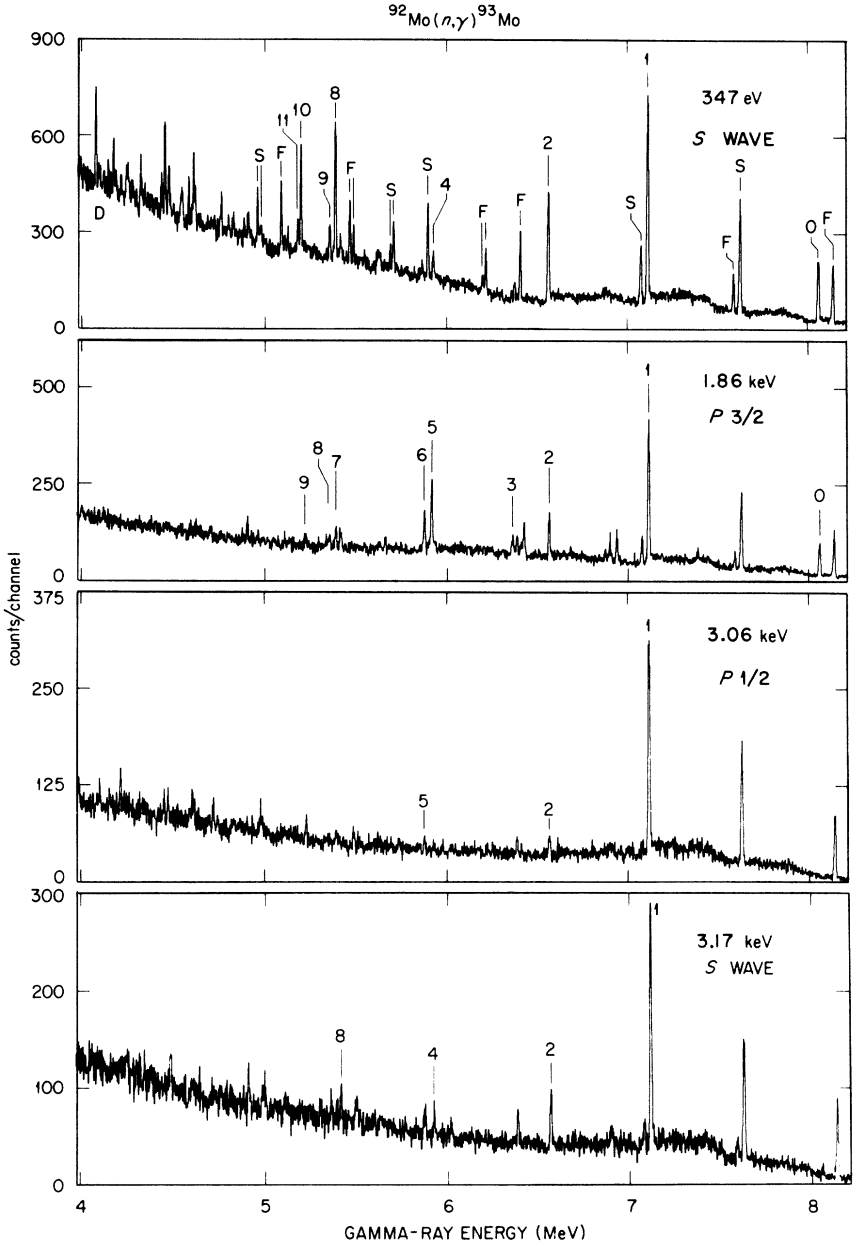

FIG. 4. Representative high-energy γ-ray spectra from four different resonances. The numbers label the double-escape peaks while the letters indicate the total-energy and single-escape peaks. Peak 0 indicates the ground-state γ ray.

For this energy region the detector response yields three peaks for each γ ray. The peaks labeled with numbers indicate the two-photon escape peaks. The peak labeled 0 indicates the ground-state γ ray. A total of 12 γ rays with energies exceeding 5 MeV were observed and assigned as primary transitions from the resonances on the basis of the observed increase in γ-ray energy with increasing neutron energy. Nearly all of the 23 resolved spectra are dominated by the 7126-keV γ ray which populates the first excited state. It is this γ ray which will receive special analysis.

The 347-eV resonance spectrum shown at the top of Fig. 4 is unusual in that it contains much γ-ray strength below 5.5 MeV. Such strength is missing in the lower spectra, which are more typical of the remaining spectra.

Another interesting effect is the similarity of the spectra from the 3.17-keV s-wave resonance and the 3.06-keV p-wave resonance. The strong transitions are of $M1$ multipolarity for the s-wave resonance and $E1$ from the p wave. Such similarities indicate the near equivalence of the average $E1$ and $M1$ radiation widths which will be discussed more completely later. The spectrum from the 3.17-keV resonance has been corrected for a 15% admixture of the 3.06-keV spectrum caused by neutrons which scatter in the 3.17-keV resonance, lose energy, and then are captured in the 3.06-keV resonance. The maximum neutron energy loss on scattering is 135 eV which is greater than the resonance separation of 110 eV. The amount of admixture was calculated using the measured resonance parameters in the Monte-Carlo program O5R.[21]

The ^{93}Mo energy-level diagram based on previous experiments is shown in Fig. 5. Except for the 2141-keV level, all spin assignments are from other experiments. Included are the levels observed in the (d,p) experiments of Moorhead and Moyer.[11] Their assignments of the orbital angular momentum of the captured neutron and spectroscopic factors are listed. The states populated in the present experiment by primary γ-ray transitions from the capturing states are indicated by solid triangles on the right while those states from which secondary γ-ray transitions to the ground state were observed are indicated by solid triangles on the left. There have been conflicting assignments of the spin of the 1693-keV level, but the recent work of Ball[16] establishes the spin as $\frac{5}{2}$. As a result the spectroscopic factor reported by Moorhead and Moyer has been reduced from 0.18 to 0.12.

The level at 2141 keV was observed by both primary and secondary γ rays in the present experiment. Since it was not observed in previous (d,p) experiments we have assumed a spectroscopic factor of zero in the test of the valency model. We deduce a spin of $\frac{3}{2}$ for this level from the γ-ray angular distribution of the present experiment. A level at 2145 keV was observed in the recent $(d,p\gamma)$ work of Matthews *et al.*[18] and assigned a spin of $\frac{1}{2}$. Since it is expected that all low-lying $\frac{1}{2}$, $\frac{3}{2}$, and $\frac{5}{2}$ levels should be populated, the failure to observe the 2145-keV level in the present experiment suggests a spin larger than $\frac{5}{2}$ for the 2145-keV level.

In order to deduce the spins of the neutron reso-

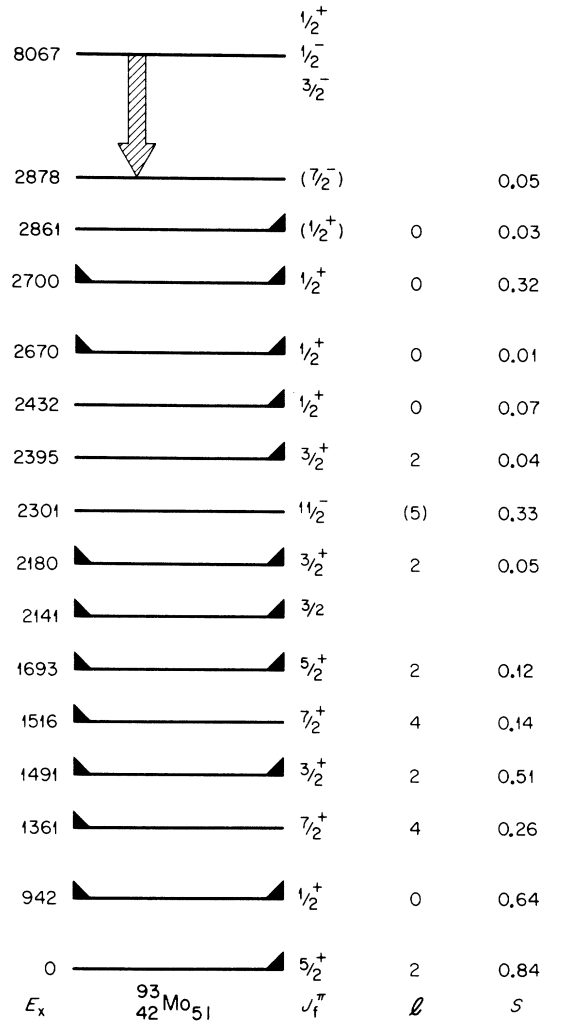

FIG. 5. Energy-level diagram of ^{93}Mo. The properties of the level at 2141 keV are from the present experiment while the remainder are from other works. The triangles on the right indicate the levels populated by primary γ rays from the capturing state while those on the left emit γ rays to the ground state. The neutron orbital angular momentum and spectroscopic factor from (d,p) reactions are shown on the right.

nances, γ-ray spectra were obtained at 90 and 140° relative to the neutron-beam direction. The γ-ray peak areas for primary transitions to final states of spin $\frac{3}{2}$ and $\frac{5}{2}$ relative to the peak area for the 7126-keV γ ray feeding the $\frac{1}{2}^+$ state at 942 keV were observed at both angles. This ratio is constant with angle for resonances of spin $\frac{1}{2}$ but changes for spin-$\frac{3}{2}$ resonances. The results of this measurement are listed in Table III for those resonances for which the γ rays were strong enough to be useful for resonance spin assignments. Shown are the experimental values of the ratio $R(J_f)$ defined as

$$R(J_f)=\frac{[A(J_f)/A(7126)]_{140°}}{[A(J_f)/A(7126)]_{90°}}.$$

For pure dipole γ rays this ratio is unity for spin-$\frac{1}{2}$ resonances, and is given by

$$R(\tfrac{3}{2})=2.28$$

and

$$R(\tfrac{5}{2})=1.43$$

for spin-$\frac{3}{2}$ resonances. Resonances for which the ratios are consistent with unity are assigned spin $\frac{1}{2}$ while those which are consistent with 1.43 or 2.28 are assigned spin $\frac{3}{2}$. The method yields definite spin assignments for six resonances. The results for three other resonances are marginal and the resulting spin assignments are enclosed in parentheses. The spins of $\frac{1}{2}$ for the 0.347-, 3.17-, and 6.8-keV resonances are in agreement with the values from the neutron-transmission measurements.[9]

There are conflicting measurements of the spin of the 5.6-keV resonance. The nearly isotropic angular-distribution measurement indicates a spin of $\frac{1}{2}$ while the γ-ray spectrum indicates spin $\frac{3}{2}$. The γ ray populating the $\frac{5}{2}^+$ ground state in this resonance is one of the strongest observed. Since the neutron-transmission experiment[9] requires the resonance parity to be negative, a $\frac{1}{2}^-$ assignment requires this γ ray to be an $M2$ or $E3$ multipole which we consider improbable. Thus the γ-ray spectral measurement strongly suggests an $E1$ multipolarity and a resonance spin of $\frac{3}{2}$. Possible sources of distortion of the angular-distribution measurement are multiple neutron scattering in the resonance and a multipole admixture in the γ-ray widths. However, multiple neutron scattering in this resonance is not sufficient to weaken an anisotropic angular distribution since the multiple scattering is larger in the 4.3-keV resonance where the anisotropy is strong. A 1% $M2$ admixture in both the γ-ray decay to the ground state and first excited state is sufficient to produce the experimental result for a $p_{3/2}$ resonance. The transition to the $\frac{5}{2}^+$ ground state is more sensitive to the γ-ray mixing ratio than transitions to the $\frac{3}{2}^+$ final states. Such a large $M2$ width is perhaps not unusual in this nucleus which has enhanced $M1$ and $E2$ widths. We thus conclude that the spin and parity of the 5.6-keV resonance is $\frac{3}{2}^-$ and that the small anisotropy observed in the γ-ray angular distribution is possibly a result of an $M2/E1$ admixture of γ-ray multipolarities.

From the angular-distribution measurement we

TABLE III. γ-ray angular-distribution results. The deduced value of the resonance spin is given in column 2. The experimental γ-ray intensity ratio is given by $R(J_f)=[A(J_f)/A(7129)]_{140°}/[A(J_f)/A(7129)]_{90°}$. The theoretical value for pure $E1$ γ rays is $R=1.0$ for $J_\lambda=\frac{1}{2}$. For $J_\lambda=\frac{3}{2}$ the values are $R(\frac{3}{2})=2.2$ and $R(\frac{5}{2})=1.4$.

		$R(J_f)$				
E_r (keV)	J_λ	$\frac{5}{2}^+$ 8067	$\frac{3}{2}^+$ 6577	$\frac{3}{2}^+$ 5928	$\frac{3}{2}^+$ 5891	$\frac{3}{2}^+$ 5672
0.347	$\frac{1}{2}$	1.08±0.08	1.12±0.10			
1.9	$\frac{3}{2}$	1.25±0.20	2.4 ±0.2	1.9±0.2		
2.3	$\frac{3}{2}$	2.5 ±0.8				1.6±0.4
3.06	$(\frac{1}{2})$		1.4 ±0.5		0.9±0.4	
3.17	$\frac{1}{2}$		1.3 ±0.2		0.6±0.3	
4.3	$\frac{3}{2}$		2.1 ±0.3	3.4±0.9	3.7±1.0	
5.6	$(\frac{3}{2})$ [a]	1.03±0.20				
6.0	$\frac{3}{2}$	1.56±0.17	3.0 ±1.5	1.7±0.8		
6.8	$(\frac{1}{2})$				0.5±0.3	

[a] See text for discussion of this assignment.

TABLE IV. Partial radiation widths for 12 final states in ^{93}Mo. The neutron energies are listed in column 1. Those energies without a spin assignment contain unresolved resonances. The total radiation widths are listed in column 3. The errors in the partial widths due to the uncertainty in the γ-ray peak areas are enclosed in parenthesis.

E_n (keV)	J^π	$\Gamma_{\lambda\gamma}$ (10^{-3} eV)	$\Gamma_{\gamma\lambda f}$ (10^{-3} eV) 8067	7126.0	6575.6	6374.8	5928.0	5888.0	5671.4	5634.1	5397.6	5365.7	5207.5	5188.9
0.3	$\frac{1}{2}^+$	178	8.8(0.3)	26.0(0.4)	12.6(0.5)	0.4(0.2)	−0.2(0.3)	0.2(0.4)	−0.0(0.3)	0.9(0.3)	14.1(0.6)	2.5(0.6)	9.1(0.6)	1.3(0.5)
1.9	$\frac{3}{2}^-$	240	21.3(1.1)	73.4(1.9)	29.8(2.5)	8.0(1.7)	29.0(1.7)	23.5(2.5)	2.8(1.6)	0.6(1.0)	4.6(1.5)	2.8(1.1)	−0.7(1.0)	0.1(1.1)
2.3	$\frac{3}{2}^-$	240	6.4(1.1)	86.2(2.2)	1.7(1.5)	0.2(1.1)	2.3(1.2)	3.3(1.9)	20.6(3.5)	−0.6(1.2)	0.8(1.3)	2.9(1.4)	3.4(1.4)	0.7(1.3)
3.1	$(\frac{1}{2})^-$	240	0.2(0.3)	146.2(3.7)	6.7(1.7)	−0.2(1.2)	−1.4(1.3)	6.6(1.9)	1.1(1.3)	1.5(1.3)	0.8(1.3)	−0.8(1.3)	−0.8(1.4)	0.9(1.4)
3.2	$\frac{1}{2}^+$	210	1.9(0.7)	64.1(2.3)	16.2(2.0)	1.3(1.1)	−0.2(1.1)	10.7(2.1)	−0.3(1.3)	1.8(1.3)	0.8(1.4)	2.7(1.4)	1.1(1.5)	0.3(1.5)
4.3	$\frac{3}{2}^-$	210	0.6(0.5)	65.7(2.1)	104.0(3.6)	2.4(1.4)	5.6(1.5)	12.5(2.4)	2.7(2.2)	0.7(1.4)	0.2(1.4)	14.3(2.2)	1.3(1.4)	−1.2(1.6)
5.6	$(\frac{3}{2})^-$	300	143.0(4.6)	54.1(3.5)	8.4(4.8)	10.8(3.4)	4.0(2.6)	3.7(2.9)	0.1(3.2)	2.2(2.0)	−0.1(2.0)	3.1(2.3)	−1.0(2.2)	−0.8(2.0)
6.0	$\frac{3}{2}^-$	340	69.1(4.1)	166.2(5.5)	11.5(4.5)	−0.7(3.3)	18.4(3.5)	7.6(5.1)	11.9(4.1)	4.6(3.1)	0.4(2.9)	15.2(4.3)	1.9(3.3)	−1.3(3.3)
6.4	$(\frac{1}{2})^-$	97	9.4(2.0)	12.4(2.4)	0.2(1.6)	0.8(1.9)	1.6(1.7)	1.9(1.9)	0.2(2.5)	21.2(3.5)	4.3(2.6)	1.8(2.6)	2.9(2.7)	0.1(2.7)
6.8	$\frac{1}{2}^+$	159	1.5(1.3)	16.1(3.4)	2.3(2.0)	0.4(2.3)	5.2(2.7)	30.9(4.5)	3.1(2.8)	2.9(2.6)	0.7(2.8)	40.9(5.8)	3.5(2.9)	0.2(2.9)
7.1	$\frac{1}{2}^+$	150	2.5(1.2)	3.4(2.2)	4.3(2.1)	−1.1(2.1)	29.2(4.0)	14.2(2.4)	1.5(2.7)	4.0(2.8)	3.4(3.1)	7.9(3.4)	−0.4(3.2)	5.0(3.5)
8.8		240	16.2(2.2)	69.5(4.7)	38.7(5.1)	35.8(4.7)	4.9(3.0)	7.2(3.3)	6.0(3.5)	3.5(3.6)	−0.3(3.7)	19.8(5.1)	0.7(3.8)	−1.3(3.8)
9.2	$(\frac{1}{2})^-$	200	1.2(1.9)	44.2(5.0)	91.3(6.6)	6.9(4.2)	3.8(4.5)	2.9(4.6)	−4.3(4.6)	31.8(6.3)	2.1(4.7)	9.1(5.0)	3.2(4.8)	2.6(4.8)
10.6	$\frac{3}{2}^-$	290	52.3(4.3)	9.7(3.3)	66.2(8.3)	2.5(4.4)	23.0(6.1)	3.0(6.6)	3.2(5.9)	7.5(4.3)	−1.0(4.7)	4.4(4.7)	0.5(4.9)	−0.4(5.3)
11.0	$(\frac{3}{2})^-$	240	17.8(3.1)	10.6(3.3)	8.5(5.8)	0.8(3.2)	1.6(2.7)	−0.9(4.9)	2.5(4.4)	1.2(3.2)	0.2(3.2)	6.5(3.2)	4.6(3.3)	1.2(3.3)
11.6	$\frac{1}{2}^+$	185	6.1(4.1)	32.8(7.2)	4.2(6.2)	1.3(6.2)	1.8(6.3)	3.6(6.4)	−3.2(6.5)	−1.2(6.5)	−2.8(6.5)	17.8(9.5)	1.0(8.4)	1.0(7.5)
12.8	$\frac{3}{2}^-$	240	87.8(5.8)	54.5(4.4)	2.3(3.2)	7.5(2.5)	−0.5(2.0)	1.0(3.3)	8.3(3.3)	0.4(2.1)	2.9(2.1)	3.9(2.6)	1.3(2.5)	0.1(2.6)
13.8	$\frac{1}{2}^+$	132	6.1(4.3)	7.4(5.1)	2.8(5.3)	2.3(5.7)	2.3(5.9)	1.5(6.6)	5.2(7.4)	6.0(6.7)	1.6(7.1)	1.3(7.4)	0.5(7.6)	−0.8(7.7)
14.2	$(\frac{1}{2})^-$	155	8.9(4.7)	12.1(5.1)	36.2(7.0)	1.7(5.2)	4.5(7.0)	1.8(5.4)	6.7(7.3)	1.3(7.3)	−0.8(7.3)	8.5(7.3)	1.3(7.5)	2.7(7.6)
14.5	$\frac{3}{2}^-$	240	28.2(5.8)	29.6(5.8)	9.8(6.9)	−1.4(5.0)	2.2(5.6)	0.3(6.9)	23.3(9.0)	−0.8(4.8)	−1.0(5.2)	6.2(5.2)	−0.4(5.7)	4.5(6.8)
15.6		240	6.1(2.6)	11.5(4.5)	11.0(3.9)	14.9(3.9)	7.8(4.4)	4.4(4.1)	1.2(4.1)	3.7(4.3)	−2.0(4.6)	2.1(4.6)	2.4(4.7)	−0.2(3.9)
16.5	$\frac{1}{2}^+$	166	0.4(4.8)	13.0(7.7)	0.4(6.8)	2.8(8.5)	14.2(10.5)	2.9(9.8)	3.7(10.9)	7.0(10.9)	4.4(10.5)	7.8(11.8)	−3.0(12.2)	−0.4(12.3)
17.2	$\frac{3}{2}^-$	380	9.2(6.9)	5.7(8.5)	−1.3(18.1)	112.6(21.1)	22.9(15.3)	−7.6(19.6)	15.4(19.8)	0.9(12.7)	−6.3(12.7)	−3.6(12.7)	13.9(12.1)	−8.4(15.0)
18.1		240	10.0(3.4)	0.6(4.0)	16.4(4.5)	10.3(4.7)	0.2(4.3)	14.6(5.9)	4.9(5.1)	8.7(5.1)	8.6(5.9)	−1.4(5.1)	0.3(5.2)	1.8(5.4)
19.2	$(\frac{3}{2})^-$	180	9.1(3.8)	10.8(4.6)	3.7(7.4)	2.6(5.6)	32.8(8.7)	−3.0(7.6)	2.2(7.7)	8.4(4.9)	8.4(5.0)	13.9(5.0)	5.4(5.8)	−3.3(5.8)
20.6		150	18.7(8.7)	28.2(10.5)	22.3(14.9)	5.5(10.3)	21.0(13.4)	9.3(10.6)	−9.1(10.7)	14.8(13.0)	−4.6(13.1)	14.9(8.6)	17.8(15.5)	−7.3(11.2)
21.4		177	6.4(2.8)	4.8(3.6)	3.3(3.3)	4.8(4.4)	−0.2(4.2)	0.7(4.9)	3.7(4.9)	2.6(4.9)	−1.4(5.0)	3.9(5.0)	−2.0(5.1)	5.6(5.1)
22.1		240	197.5(12.9)	39.4(9.1)	1.9(7.9)	2.5(7.9)	2.2(8.9)	2.9(9.2)	−3.5(9.3)	3.8(9.3)	−0.3(10.3)	12.2(10.3)	0.6(10.6)	3.6(10.3)
23.9	$(\frac{3}{2})^-$	350	16.3(5.9)	204.4(12.7)	12.9(13.3)	13.7(10.2)	0.8(7.2)	−3.2(13.8)	−6.9(13.9)	10.3(9.7)	4.0(9.7)	9.9(10.4)	−2.6(9.3)	3.3(9.3)

have clearly determined the spins of four p-wave resonances which are not known by any other method. This measurement also agrees with the spin-$\frac{1}{2}$ assignment for three s-wave resonances deduced from the neutron-transmission measurement.[9]

Additional resonance spin assignments are based on the observation of a "strong" transition to the $\frac{5}{2}^+$ ground state and 1693-keV state. It is assumed that these strong transitions are $E1$ and thus come from $\frac{3}{2}^-$ resonances. This technique must be used with caution since an $E2$ transition is observed in the 346-eV s-wave resonance. On this basis we assign a spin and parity of $\frac{3}{2}^-$ to the resonances at 12.8 and 17.2 keV.

The partial radiation widths of the high-energy γ rays deduced for each γ-ray spectrum are listed in Table IV for neutron energies less than 25 keV. The neutron energies and resonance spins and parities are listed in columns 1 and 2, respectively. No spin assignments are listed for unresolved resonances. The listed spin assignments are from the present work and the work of Ref. 9. Assignments deduced from the values of $g\Gamma_\gamma$ are enclosed in parentheses and are less certain. The total radiation widths used in Eq. (4) to determine the partial widths are listed in column 3. The 18 values determined from the total capture and transmission experiment[9] are shown. The unknown widths are assigned a value of 170 meV for s waves and 240 meV for p waves, which are approximately the average radiation widths. It is estimated that this assumption can introduce a maximum 50% systematic error in the partial widths. The deduced partial radiation widths in units of milli-electron volts are listed in the remaining columns. The errors from the uncertainty in the net γ-ray peak areas are enclosed in parentheses. The radiation widths of the 5.6-, 6.0-, and 23.9-keV resonances, which are much larger than the mean value, have an uncertainty of approximately 50%, which produces an uncertainty of 50% in the partial radiation widths of these resonances. It is also these three resonances which contain the strongest γ-ray partial widths. The systematic error in the remaining resonances with measured total radiation widths is estimated to be 25%. The observation of large total radiation widths for resonances which contain a few strong high-energy γ rays is expected since the summed strength of the lower-energy primary γ rays is expected to be nearly constant because of the statistical distribution of these widths.

Inspection of the table shows that the three highest-energy γ rays contain the dominant strength for most of the resonances. This is the trend predicted by the valency model which will be further investigated in the following section.

VI. DISCUSSION

A. Valency-Model Comparison

The valency model of neutron capture predicts that the γ-ray decay widths are proportional to the reduced neutron widths of both the capturing and final states. As is indicated in Fig. 5, the largest final-state neutron widths are in the lowest energy levels as indicated by the large spectroscopic factors. The valency transitions are thus predicted to be strong for transitions to the $\frac{5}{2}^+$ ground state,

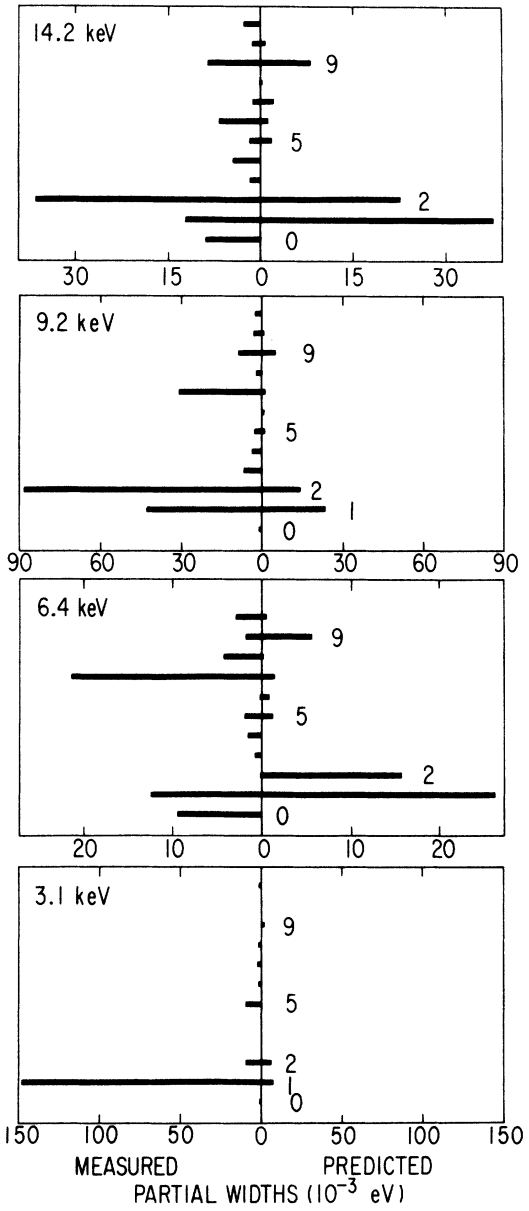

FIG. 6. Comparison of the observed γ-ray widths with those predicted by the valency model for $p_{1/2}$ resonances.

the $\frac{1}{2}^+$ first excited state, and the $\frac{3}{2}^+$ state at 1491 keV excitation. The extreme statistical model, on the other hand, predicts no such dependence. We therefore expect that the γ-ray transition probability contains contributions from both processes and we thus write for the observed width,

$$\Gamma_{\gamma\lambda J} = |\Gamma^{1/2}_{\gamma\lambda J}(SP) + S\Gamma^{1/2}_{\gamma\lambda J}|^2 .$$

The phases of the single-particle amplitude and the non-valency-model amplitude, $S\Gamma^{1/2}_{\gamma\lambda J}$, can vary so that the two amplitudes may interfere constructively or destructively. This effect precludes the possibility of extracting the two amplitudes directly from the observed widths for individual resonances. However, for widths averaged over many resonances we expect the net interference effects to be small and thus to be able to determine the relative average size of the single particle and nonvalency widths.

The valency-model predictions given by Eq. (1) apply only to $E1$ γ rays, which are observed only from the p-wave resonances. Since the low-lying states in ^{93}Mo populated in the present experiment are all positive parity, the high-energy γ rays from the s-wave resonances are either $M1$ or $E2$ transitions. We shall exclude the s-wave reso-

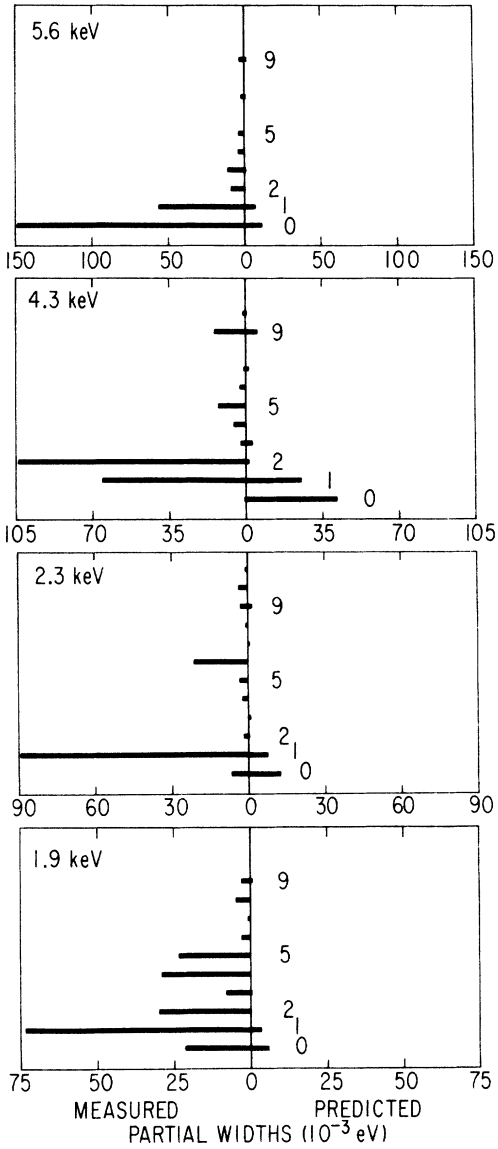

FIG. 7. Comparison of observed and predicted γ-ray widths for $p_{3/2}$ resonances.

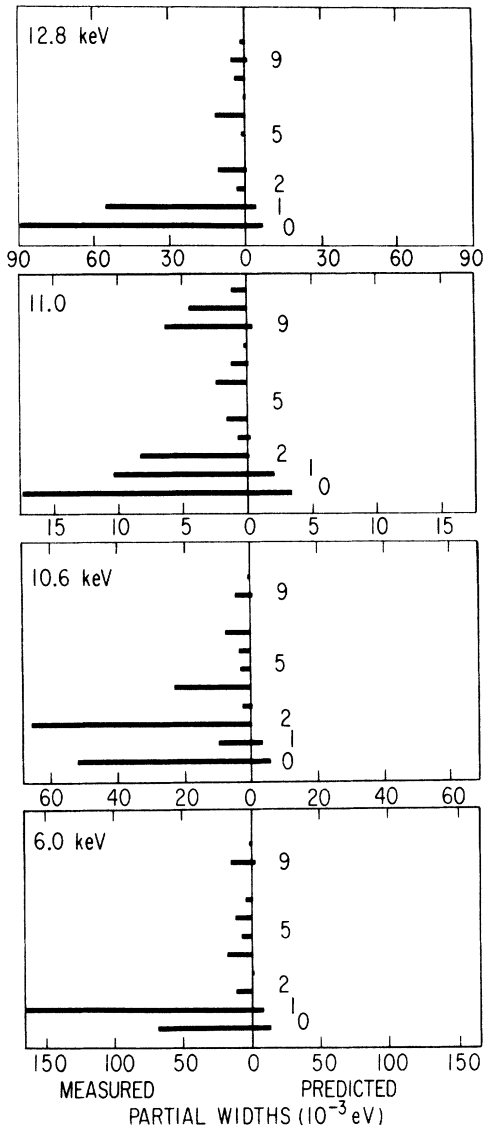

FIG. 8. Observed and predicted widths for $p_{3/2}$ resonances.

nances from the discussion and concentrate on the p-wave resonances.

A comparison of the observed widths with those predicted by the valency model of Eq. (1) are shown in Fig. 6 for the four lowest energy-resolved $p_{1/2}$ resonances. The resonant reduced p-wave neutron widths listed in Ref. 9 are used in the calculation. The observed widths are shown on the left while the predicted widths are on the right. The bars labeled 0 indicate the ground-state γ rays. There is little detailed agreement, although the trend for concentration of strength in the low-lying states is observed in both experiment and prediction.

A similar comparison for 12 $p_{3/2}$ resonances is given in Figs. 7–9. Again there is little detailed agreement, although the high-energy γ rays are strong. The predicted widths tend to be smaller than the observed widths. The spectra which yield the best detailed agreement with the model are the 15.6- and 8.8-keV spectra shown in Fig. 10. These spectra are from unresolved doublets. In the calculation, resonances of both spins were assumed to contribute in the ratio of their neutron widths ($g\Gamma_n$) in both spectra. The reduced neutron widths of the 8.8-keV doublet, which are 2.1 and 1.0 eV,[9] are the strongest while those from the 15.6-keV doublet are of average strength. The valency-model prediction of the summed intensity of the 12 γ rays in the 8.8-keV doublet is 60% of the observed sum, which is the largest fractional contribution of any spectrum. However, the partial widths of the 8.8-keV doublet are not exceptionally large.

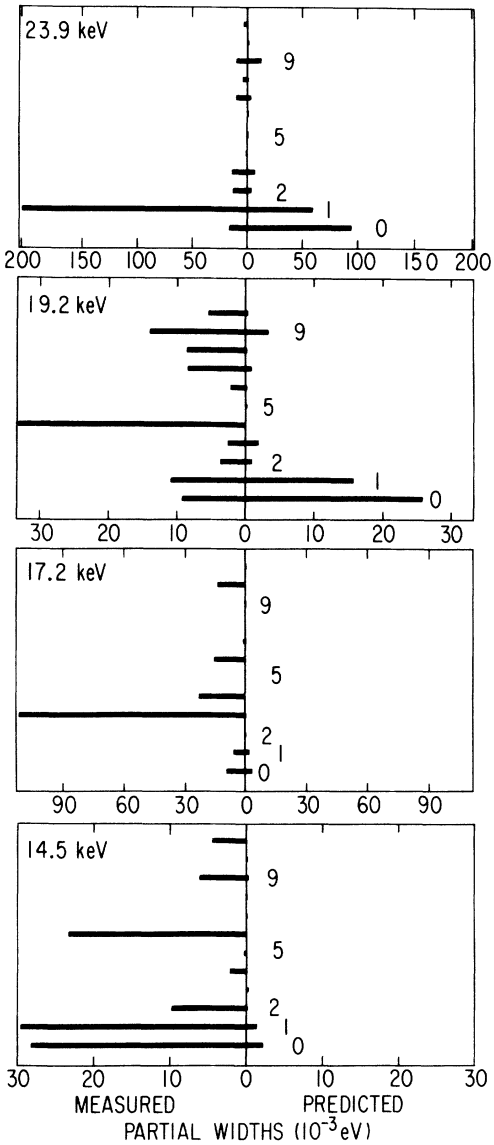

FIG. 9. Observed and predicted widths for $p_{3/2}$ resonances.

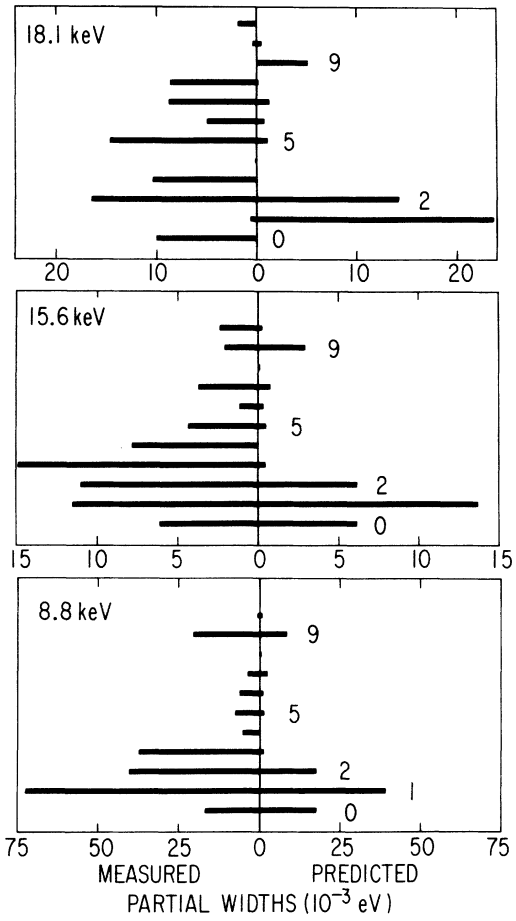

FIG. 10. Observed and predicted widths for unresolved resonances.

Thus, the agreement between the valency model and experiment for these two spectra is considered fortuitous and not a significant result.

A detailed comparison of the predicted and observed widths for the three highest-energy γ rays which contain most of the predicted model strength shows that the general trend is for the predicted widths to be smaller than the observed widths. No correlation is found between the observed widths and the reduced neutron widths of the resonance for the 8067- and 6576-keV γ rays. However, positive correlation is suggested for the 7126-keV γ ray. This topic will be pursued in a later section. We conclude from this comparison that the valency model does not produce the dominant contribution to the observed partial radiation widths.

B. Average Partial Widths

In order to further determine the average size of the valency-model contribution to the partial widths we refer to the average partial widths. The average partial widths for the resolved resonances are shown in Fig. 11 for the s- and p-wave resonances. Due to the small number of $p_{1/2}$ resonances, both p-wave spins are placed in a single group. The open bars indicate the average widths for sample size of 7 s-wave, 12 p-wave for $\frac{5}{2}$ final states, and 16 p-wave resonances for the remaining final states. The solid bars in the p-wave graphs indicate the average valency-model predictions for the three highest-energy γ rays. The valency-model predictions are insignificant for the lower-energy γ rays and are not shown. The γ-ray widths for $E_\gamma > 6.4$ MeV are clearly stronger than those at lower energies for each group.

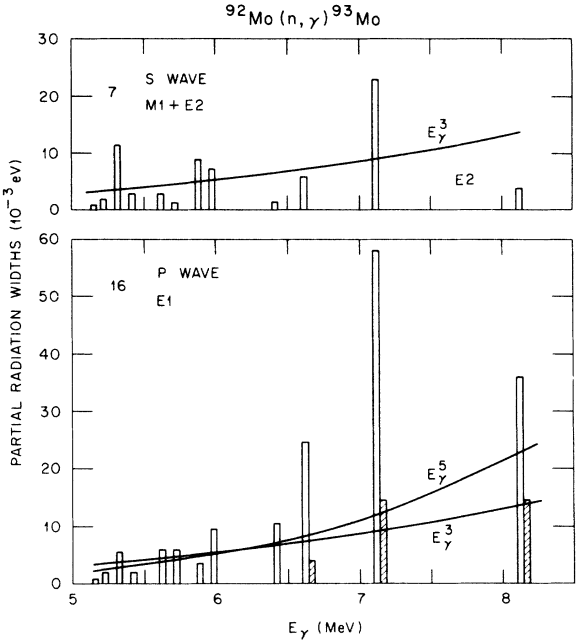

FIG. 11. Average partial radiation widths for s-wave and p-wave resolved resonances. The γ rays in the s-wave spectrum are of $M1/E2$ multipolarity while those in the p-wave spectrum are $E1$. The average $E1$ widths for the p-wave resonances include 12 resonances for the two $\frac{5}{2}$ final states and 16 resonances for the $\frac{1}{2}$ and $\frac{3}{2}$ final states while seven resonances are included for the s-wave average widths.

In order to measure the enhancement we shall assume that the γ-ray transitions for $E_\gamma < 6.4$ MeV follow a simple statistical model for which the average reduced matrix element is energy-independent. For this case we have

$$\langle \Gamma_{\lambda f} \rangle_\lambda \propto E_\gamma^3 .$$

We arbitrarily normalize these intensities to 5.19 MeV and obtain for the average normalized width the values 3.4 ± 0.6 and 3.6 ± 0.4 meV for the s- and p-wave spectra, respectively, which agree within the listed error. The errors result from assuming a Porter-Thomas distribution of partial widths. The smooth curves in Fig. 11 show the energy dependence of the γ-ray widths for the E_γ^3 law extrapolated from the average value below 6.4 MeV.

For the $E1$ γ-ray widths from the p-wave spectra, we immediately observe that the three γ-ray transitions with energies exceeding 6.5 MeV are much stronger than predicted by the E_γ^3 law. We also observe that the calculated valency-model contribution to the average partial width is approximately 40%, 25%, and 15% for the 8067-, 7126-, and 6576-keV γ rays, respectively. This agrees with the conclusion from the individual spectra that the valency contribution is not the dominant part of the observed partial radiation widths. For the 8067-keV ground-state γ ray the enhancement above the E_γ^3 line is consistent with the valency-model prediction. However, for the 7126- and 6576-keV γ rays the valency prediction accounts for only approximately 35% of the enhancement over the E_γ^3 dependence. We thus conclude that the valency-model contribution to the neutron-capture reaction mechanism is sufficient to explain the enhanced γ-ray strength for the ground-state γ ray but not the strength to the first excited $\frac{1}{2}^+$ and $\frac{3}{2}^+$ states.

One way, of course, to increase the predicted valency-model partial widths is to change some of the parameters used in the calculation, such as the effective charge of the neutron or the size of the Wigner limit for the neutron widths. Let us suppose that by a suitable choice of parameters we increase the predicted size of the partial widths

by a factor of 4 so that the enhancement of the 7126-keV γ ray is entirely explained by the valency model. Since the valency model predicts that the partial width is proportional to the reduced neutron width of the resonance, one expects to observe a correlation coefficient of unity between the partial radiation widths and reduced neutron widths of the resonances. The correlation coefficient ρ is defined by

$$\rho = \frac{\sum_\lambda (\Gamma_{\lambda f} - \langle \Gamma_{\lambda f} \rangle)(\Gamma^1_{n\lambda} - \langle \Gamma^1_{n\lambda} \rangle)}{\left[\sum_\lambda (\Gamma_{\lambda f} - \langle \Gamma_{\lambda f} \rangle)^2 \sum_\lambda (\Gamma^1_{n\lambda} - \langle \Gamma^1_{n\lambda} \rangle)^2\right]^{1/2}}.$$

A plot of the observed partial radiation widths and the resonant reduced neutron widths for the 7126-keV γ ray is shown in Fig. 12. We have included all of the widths listed in Table IV. This includes the six groups of unresolved p-wave resonances as well as the 16 resolved p-wave resonances. The error bars on the points do not include a possible factor-of-2 systematic error due to the uncertainty in some spin assignments. The correlation coefficient is +0.51 and is indicated by the regression line shown in the figure. The correlation is due largely to the large widths of the 23.9-keV resonance. The scatter of the data is much larger than expected if the average valency-model width is 5 times the average statistical-model width. The scatter is, however, consistent with a smaller ratio of the average valency width to the average statistical width. The small correlation between the observed partial widths and the resonance reduced neutron width is evidence against a possible factor-of-4 increase in the predicted size of the valency-model width for the 7126-keV γ ray. We thus conclude that the enhanced strength of the 7126-keV γ ray cannot be explained entirely by the valency-model contribution.

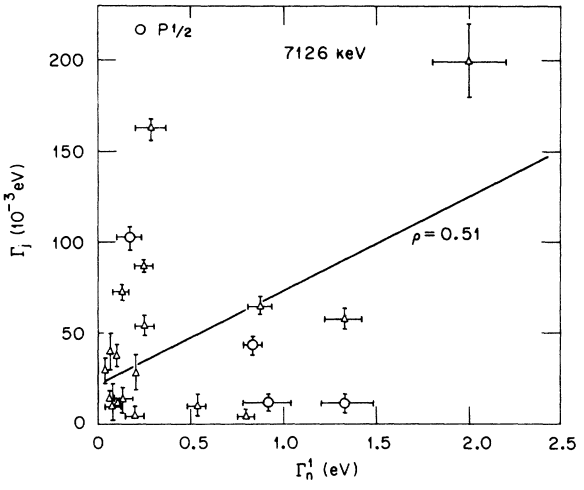

FIG. 12. Comparison of the observed partial radiation width of the 7126-keV γ ray with the reduced p-wave neutron width of each resonance. The open circles indicate resonances of known spin $\frac{1}{2}$ while a spin of $\frac{3}{2}$ is used for the resonances indicated by triangles. A regression line for the correlation coefficient of +0.51 is shown.

As a further test of the valency-model contribution to the partial radiation widths, we have calculated the correlation coefficients between the partial radiation widths and the resonant reduced neutron widths for all of the γ rays for both the s- and p-wave resonances. The only case in which the correlation coefficient is large enough to be statistically significant is the 7126-keV γ ray in the p-wave resonances. Of course one does not expect to observe a correlation for the $M1$ transitions from the s-wave resonances. The small correlation coefficients for the remainder of the $E1$ transitions is consistent with the previous predictions of the small size of the valency-model contributions.

C. Photon Strength Function

One of the means of cataloging the average partial radiation widths is the photon strength function which is defined by Bartholomew[25] for $E1$, $M1$, and $E2$ transitions as

$$k(E1) = \langle \Gamma_{\lambda f}(E1) \rangle / E_\gamma^3 D A^{2/3},$$

$$k(M1) = \langle \Gamma_{\lambda f}(M1) \rangle / E_\gamma^3 D,$$

$$k(E2) = \langle \Gamma_{\lambda f}(E2) \rangle / E_\gamma^5 D A^{4/3},$$

where the radiative widths are in units of electron volts, D is the average spacing of neutron resonances of same spin and parity (in MeV), A is the nuclear mass number, and E_γ is in MeV. The strength functions obtained from the present experiment are listed in Table V. The electric quadrupole strength function is obtained from the transitions to the two $\frac{5}{2}^+$ final states populated from the seven s-wave resonances. The $M1$ strength function is obtained from the average of the nine γ rays with energies less than 7.0 MeV from the seven s-wave resonances. These widths were assumed to be pure $M1$ transitions. The 7126-keV γ ray is listed separately since it is stronger than the other transitions. The $E1$ strength function is calculated from the 16 resolved p-wave resonances. The three highest-energy γ rays with enhanced strength are listed separately from the lower-energy γ rays. The listed errors result from the assumption of the Porter-Thomas distribution for the individual γ rays.

The amount of existing data on $E2$ widths for this energy interval for this mass region is rather lim-

ited. Thus there is nothing meaningful with which to compare the observed strength function. However, the average $E2$ partial width for the 8067-keV γ ray is approximately $\frac{1}{10}$ of the average $E1$ partial width for this γ ray. This suggests a very large enhanced $E2$ width since this is approximately 100 times the ratio predicted by the Weisskopf units.

The $M1$ strength function is large compared to the average values of all nuclei listed in the Bartholomew compilation.[25] The data in Table V strongly indicate that the average 7126-keV $M1$ strength is enhanced by at least a factor of 2 relative to the lower-energy γ rays. However, this conclusion must be treated with caution since there is an approximately 10% probability that the 7126-keV value is equal to the lower-energy value. The average $M1$ partial widths are approximately equal to the average $E1$ partial widths for the lower-energy γ rays. This is a larger ratio than was observed by Bollinger[26] for other nuclei above mass 100 where he observed that the average $M1$ width was about $\frac{1}{5}$ of the average $E1$ width.

Now let us concentrate on the enhanced $E1$ strength of the highest-energy γ rays. The value of the strength function for the lower-energy γ rays as listed in Table V is typical of this mass region. On the other hand the 7126-keV strength function is larger by a factor of 6. The enhanced strength of the three high-energy γ rays is also sufficient to account for the fact that the average p-wave total radiation width is 40% larger than the average s-wave total radiation width.[9]

We have shown that the enhancement for the 7126- and 6575-keV γ rays cannot be satisfactorily explained on the basis of the valency model alone. Another possible mechanism is the giant-dipole-resonance model[27] which has been invoked by Bollinger and Thomas[26,28] to explain the departures from the E_γ^3 dependence of the average $E1$ γ-ray intensities for many nuclei. This model leads to an approximately E_γ^5 dependence on the average γ-ray widths for γ-ray energies in the region from 5 to 8 MeV if it is assumed that each excited state has the same giant resonance built on it. This dependence is indicated in Fig. 11. The increased average intensity predicted by this energy dependence is not sufficient to significantly change the conclusions based on the E_γ^3 law. We thus conclude that the giant-dipole-resonance contribution to the $E1$ strength function is not sufficient to explain the enhanced average strength of the high-energy γ rays in ^{93}Mo.

Another possible explanation is the doorway-state mechanism[29] applied to neutron-capture reactions by Lane[30] and Beer.[31] In this picture the two-particle–one-hole component of the neutron resonances plays a dominant role. For ^{93}Mo we prefer a particle-hole component which would not produce a correlation between the resonance neutron width and the partial radiation widths of the high-energy γ rays. One such component results if the captured p-wave neutron drops into a low-lying s- or d-wave final state while exciting a proton to an excitation of approximately 7 MeV. The proton particle-hole annihilates to emit the $E1$ γ ray of nearly 7-MeV energy. This particular process was invoked by Rimawi *et al.*[32] to explain the enhanced $E1$ γ-ray transition strengths observed for p-wave neutron capture in the neighboring target nucleus ^{94}Nb. There are sufficient proton single-particle states separated by nearly 7-MeV energy in ^{93}Mo to allow this picture to be a possibility.

However, at the present time the doorway-state concept is only of qualitative nature and lacks detailed predictability. To be consistent with the present experiment the doorway-state component must contribute approximately 30 meV (~50%) to the average partial radiation width of the 7126-keV γ ray. We must await for further developments in the field to test this model.

The enhanced strength of the 7126-keV γ ray is also consistent with the calculations of Soper[33] which suggest that $p \rightarrow s$ γ-ray transitions should be stronger than $p \rightarrow d$ transitions in this γ-ray

TABLE V. Reduced γ-ray widths in ^{93}Mo. The values for $k(E2)$ and $k(M1)$ are from the seven s-wave resonances while the values of $k(E1)$ are from the 16 resolved p-wave resonances.

Multipolarity	D (keV)	No. widths	Reduced widths
$k(E2)$	2.35	14	$(1.1 \pm 0.4) \times 10^{-7}$
$k(M1)$ $E_\gamma < 7.0$ MeV	2.35	63	$(11.5 \pm 2.3) \times 10^{-3}$
$k(M1)$ $E_\gamma = 7.126$ MeV	2.35	7	$(27.4 \pm 14.3) \times 10^{-3}$
$k(E1)$ $E_\gamma < 6.4$ MeV	1.0	144	$(1.2 \pm 0.2) \times 10^{-3}$
$k(E1)$ $E_\gamma > 6.4$ MeV	1.0	48	$(6.1 \pm 1.2) \times 10^{-3}$

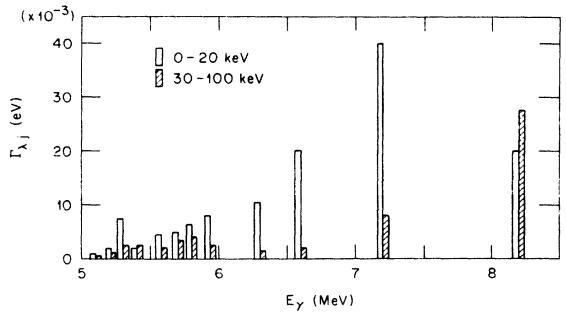

FIG. 13. Comparison of average partial widths for two different neutron-energy intervals.

energy region. In this calculation more of the p to d giant-dipole strength is shifted to higher γ-ray energies. The 7126-keV γ ray is a $p \rightarrow s$ transition while the 8067- and 6575-keV γ rays are $p \rightarrow d_{5/2}$ and $p \rightarrow d_{3/2}$ transitions, respectively. To test whether the dominance of the $p \rightarrow s$ transitions continues at higher neutron energies, we refer to Fig. 13 which compares the average partial widths for neutron energies less than 20 keV with those for neutron energies in the interval from 30 to 100 keV. The absolute numbers are not very precise but the dominance of the ground-state transitions at the higher neutron energies is significant. This suggests that the dominance of the 7126-keV $p \rightarrow s$ transition at the lower neutron energies is not a property of the giant dipole resonance, but is a property of the structure of the neutron resonances.

This discussion shows that, while the valence-neutron components are significant, additional reaction mechanisms are important for radiative neutron capture in ^{92}Mo.

VII. SUMMARY

The partial radiation widths for 12 high-energy γ rays are deduced for seven s-wave and 16 p-wave resonances for neutron energies less than 25 keV. Additional average relative widths are obtained for the unresolved resonance region up to 100 keV. The total number of neutron captures for each spectrum was determined by the usual method of summing a wide region of the γ-ray spectrum and also by a Monte Carlo calculation using the neutron resonance parameters. The two methods agreed within 25% which we interpret as an upper limit of the systematic error in the partial widths due to this source. We measured the spins of four p-wave resonances from the γ-ray angular distribution and deduced the spins of the remaining p-wave resonances from the γ-ray spectra and the value of $g\Gamma_\gamma$ from total-capture measurements.[9]

The observed partial widths were compared to the predictions of the valency model of neutron capture and were found to consistently exceed the predictions. The correlation coefficient between the $E1$ partial radiation widths and the reduced neutron widths of the resonance yielded a positive value of statistical significance only for the 7126-keV $p \rightarrow s$ transitions. Also no correlation was observed for the $M1$ transitions. This confirms that the valency-model components are not the major source of the radiative capture mechanism.

The γ-ray strength function as defined by Bartholomew shows enhanced strength for γ-ray energies near 7 MeV for $E1$ γ rays. Approximately 35% of this enhancement is attributed to the valency model while the remainder must be associated with other mechanisms which are uncorrelated with the resonant reduced neutron widths. The enhancement exceeds that predicted by the usual extrapolation of the giant dipole resonance which assumes a similar resonance shape for each excited state. A possible source is the doorway-state component which has been invoked for p-wave neutron capture in neighboring nuclei. The qualitative features of this concept agree with the average trends although a true test must await detailed predictions. The enhancement of the $p \rightarrow s$ transitions also suggests that the low-lying states in ^{93}Mo have different giant resonances constructed on them.

The average reduced $M1$ partial width is approximately 4× the average of most nuclei while the reduced $E1$ width is of average strength. The average $E2$ width of the 8067-keV ground-state transition is approximately 10% of the average $E1$ ground-state width. This is nearly 100 times the Weisskopf-unit ratio.

We thus conclude that the valency-model contribution to the p-wave radiation capture mechanism is significant but not dominant.

ACKNOWLWDGMENTS

The authors thank A. M. Lane, S. F. Mughabghab, and R. E. Chrien for interesting and helpful discussions.

†Research sponsored by the U. S. Atomic Energy Commission under contract with the Union Carbide Corporation.

[1]S. F. Mughabghab, R. E. Chrien, O. A. Wasson, G. W. Cole, and M. R. Bhat, Phys. Rev. Lett. 26, 1118 (1971).
[2]A. M. Lane and J. E. Lynn, Nucl. Phys. 17, 586 (1960).

[3]J. E. Lynn, *Theory of Neutron Resonance Reactions* (Clarendon Press, Oxford, England, 1968).
[4]R. E. Chrien, in *Statistical Properties of Nuclei*, edited by J. B. Garg (Plenum, New York, 1972), p. 233.
[5]S. F. Mughabghab, W. R. Kane, and R. F. Casten, to be published.
[6]S. F. Mughabghab, G. W. Cole, R. E. Chrien, M. R. Bhat, O. A. Wasson, and G. G Slaughter, Bull. Am. Phys. Soc. 17, 16 (1972).
[7]N. C. Pering and T. A. Lewis, IEEE Trans. Nucl. Sci. NS16, 316 (1969).
[8]T. Teichman and E. P. Wigner, Phys. Rev. 87, 123 (1952).
[9]O. A. Wasson, B. J. Allen, R. R. Winters, R. L. Macklin, and J. A. Harvey, Phys. Rev. C 7, 1532 (1973).
[10]S. A. Hjorth and B. L. Cohen, Phys. Rev. 135, B920 (1964).
[11]J. B. Moorhead and R. A. Moyer, Phys. Rev. 184, 1205 (1969).
[12]E. Finckh and U. Jahnke, Nucl. Phys. A111, 338 (1968).
[13]K. P. Lieb, T. Hausmann, and J. J. Kent, Phys. Rev. 182, 1341 (1969).
[14]R. C. Diehl, B. L. Cohen, R. A. Moyer, and L. H. Goldman, Phys. Rev. C 1, 2132 (1970).
[15]D. Ashery, S. Alper, A. I. Yavin, J. P. Longequene, D. Long-a-sion, and A. Giorui, Nucl. Phys. A179, 681 (1972).
[16]J. B. Ball, Phys. Lett. (to be published).
[17]R L. Kozub and D. H. Youngblood, Phys. Rev. Lett. 28, 1529 (1972).
[18]D. L. Matthews, F. F. Hopkins, P. Richard, G. W. Phillips, and C. F. Moore, Phys. Rev. C 5, 1390 (1972).
[19]G. E. Thomas, D. E. Blatchley, and L. M. Bollinger, Nucl. Instrum. Methods 56, 325 (1967).
[20]J. K. Dickens, Oak Ridge National Laboratory Report No. TM-3509, 1971 (unpublished).
[21]J. G. Sullivan, G. G. Warner, R. C. Block, and R. W. Hockenbury, Rensselaer Polytechnic Institute Report No. 328-155, 1969 (unpublished).
[22]See for example A. J. Ferguson, *Angular Correlation Methods in Gamma-Ray Spectroscopy* (North-Holland, Amsterdam, 1965).
[23]W. R. Kane, to be published.
[24]K. J. Wetzel and G. E. Thomas, Phys. Rev. C 1, 1501 (1970).
[25]G. A. Bartholomew, Ann. Rev. Nucl. Sci. 11, 259 (1961).
[26]L. M. Bollinger, in *Experimental Neutron Resonance Spectroscopy*, edited by J. A. Harvey (Academic, New York, 1970), pp. 235–335.
[27]P. Axel, Phys. Rev. 126, 671 (1962).
[28]L. M. Bollinger and G. E. Thomas, Phys. Rev. C 2, 1951 (1970).
[29]H. Feshbach, A. K. Kerman, and R. H. Lemmer, Ann. Phys. (N.Y.) 41, 230 (1967).
[30]A. M. Lane, Phys. Lett. 31B, 344 (1970); Ann. Phys. (N.Y.) 63, 171 (1971).
[31]M. Beer, Ann. Phys. (N.Y.) 65, 181 (1971).
[32]K. Rimawi, R. E. Chrien, J. B. Garg, M. R. Bhat, D. J. Garber, and O. A. Wasson, Phys. Rev. Lett. 23, 1041 (1969); R. E. Chrien, K. Rimawi, and J. B. Garg, Phys. Rev. C 3, 2054 (1971).
[33]J. M. Soper, to be published.